THE JOURNAL OF BIOLOGICAL CHEMISTRY VOL. 289, NO. 46, pp. 32339–32352, November 14, 2014
© 2014 by The American Society for Biochemistry and Molecular Biology, Inc. Published in the U.S.A.

Yeast Importin-α (Srp1) Performs Distinct Roles in the Import of Nuclear Proteins and in Targeting Proteasomes to the Nucleus*

Received for publication, May 16, 2014, and in revised form, September 24, 2014 Published, JBC Papers in Press, October 1, 2014, DOI 10.1074/jbc.M114.582023

Li Chen and Kiran Madura[1]

From the Department of Pharmacology, Robert Wood Johnson Medical School, Rutgers University, Piscataway, New Jersey 08854

Background: Srp1 imports proteins containing nuclear localization signals (NLS) into the nucleus.
Results: Srp1 can also target proteasomes to the nucleus.
Conclusion: Srp1 binds Sts1 to specifically target proteasomes to the nucleus.
Significance: The nuclear targeting of proteasomes by Srp1 is distinct from its well established role in NLS-mediated import.

Srp1 (importin-α) can translocate proteins that contain a nuclear localization signal (NLS) into the nucleus. The loss of Srp1 is lethal, although several temperature-sensitive mutants have been described. Among these mutants, *srp1-31* displays the characteristic nuclear import defect of importin-α mutants, whereas *srp1-49* shows a defect in protein degradation. We characterized these and additional *srp1* mutants to determine whether distinct mechanisms were required for intracellular proteolysis and the import of NLS-containing proteins. We determined that *srp1* mutants that failed to import NLS-containing proteins (*srp1-31* and *srp1-55*) successfully localized proteasomes to the nucleus. In contrast, *srp1* mutants that did not target proteasomes to the nucleus (*srp1-49* and *srp1-E402Q*) were able to import NLS-containing proteins. The proteasome targeting defect of specific *srp1* mutants caused stabilization of nuclear substrates and overall accumulation of multiubiquitylated proteins. Co-expression of a member of each class of *srp1* mutants corrected both the proteasome localization defect and the import of NLS-containing proteins. These findings indicate that the targeting of proteasomes to the nucleus occurs by a mechanism distinct from the Srp1-mediated import of nuclear proteins.

Nucleocytoplasmic trafficking occurs by an evolutionarily conserved mechanism (1, 2). Small proteins may freely enter the nucleus, whereas most proteins are escorted to the nuclear pore by transport factors and subsequently into the interior of the nucleus (3, 4). Srp1 is a member of the importin-α family of nuclear transporters that bind proteins bearing a nuclear localization signal (NLS)[2] (5, 6). The yeast *Saccharomyces cerevisiae* encodes a single Srp1/importin-α protein that is essential for viability (7). Srp1 binds Kap95/importin-β, a member of a family of proteins that promotes the entry of diverse proteins into the nucleus (8). Other transporters that resemble Kap95/importin-β can import cargo independently of Srp1/importin-α (9). Nucleo-cytoplasmic trafficking is regulated by the Ran protein, which oscillates through a GTP/GDP cycle (2, 10). Srp1 is detected in the cytosol, in the nuclear pore fraction, and in punctate foci at the nuclear periphery (11), reflecting its reversible entry and exit from the nucleus.

SRP1 encodes a protein of 542 amino acid residues that comprise three distinct domains, including an amino-terminal importin-β binding (IBB) domain, a central armadillo repeat motif (ARM) (7), and a carboxyl-terminal Cse1-binding sequence (Fig. 1). The array of 10 ~40-residue ARMs in the central region of Srp1 forms the NLS-binding region. ARM-2 to -4 form a major NLS-binding domain, and ARM-7 to -8 generate a minor NLS-binding motif (12). The IBB contains a cryptic NLS motif that can bind the NLS-binding surface and exert an autoinhibitory effect (13). This interaction allows the IBB to regulate Srp1/substrate interaction and also promotes the release of cargo inside the nucleus (14). Mutation of key basic residues reduces IBB interaction with the NLS binding surface and decreases the autoinhibitory effect. The carboxyl terminus of Srp1 interacts with Cse1 to promote substrate dissociation inside the nucleus and nuclear export of Srp1 (15).

SRP1 was first characterized as a suppressor of a polymerase I temperature-sensitive mutation (11). A number of recessive and dominant mutants of Srp1 were subsequently isolated and found to contribute to multiple nuclear activities (7). Intriguingly, the amino acid changes in these mutants occurred predominantly in the ARM repeats. One exception is *srp1-31*, in which the mutation (S116F) is present in an incomplete boundary ARM that does not contact residues in NLS. Despite its well characterized requirement in nuclear import (8), *srp1* mutants have disparate effects. Specific *srp1* mutants were found to harbor defects in either nucleolar structure or RNA synthesis (7), suggesting functions that are unrelated to nuclear trafficking. Indeed, import-independent roles for importin-α have been described recently (16, 17).

* This work was supported, in whole or in part, by National Institutes of Health (NIH), NCI, Grant CA083875 and NIH Grant GM104968 (to K. M.). K. M. is the Founding President and CEO of CellXplore, Inc., which is characterizing the ubiquitin-proteasome system to develop diagnostic assays for human breast cancer; also an inventor on multiple patents.
[1] To whom correspondence should be addressed: Dept. of Pharmacology, Robert Wood Johnson Medical School, Rutgers University, 683 Hoes Lane, SPH #383, Piscataway, NJ 08854. Tel.: 732-235-5602; Fax: 732-235-4783; E-mail: maduraki@rwjms.rutgers.edu.
[2] The abbreviations used are: NLS, nuclear localization signal(s); IBB, importin-β binding; ARM, armadillo repeat motif; Tricine, *N*-[2-hydroxy-1,1-bis(hydroxymethyl)ethyl]glycine.

Targeted mutations were generated in *SRP1* (18, 19) to investigate the role of nuclear import in cell cycle progression. Amino acid substitutions were engineered in the IBB domain (*srp1-55*) and in the bipartite NLS (*srp1-E402Q*) (19, 20). These studies showed that a defect in nuclear import involving both the autoinhibitory domain and the bipartite NLS caused cell cycle-specific defects.

The growth defects of *srp1-31* and *srp1-49* are suppressed by co-expressing both mutant proteins (21), providing compelling evidence that Srp1 has multiple functions. To investigate the divergent roles of Srp1, Tabb *et al.* (21) performed a genetic study that yielded Sts1 as a dosage suppressor of *srp1-49*. Significantly, Sts1 did not suppress the growth defect of *srp1-31* (21). Sts1 is required for RNA polymerase I transcription (11), 3′ mRNA processing (22), endoplasmic reticulum/Golgi transport (23), and nuclear segregation and division (24).

Sts1 lacks distinctive structural features that could aid in understanding its biochemical role. Although it was unclear how Sts1 suppressed the proteolytic defect of *srp1-49*, it is thought to arise from a failure to import proteasomes into the nucleus (25). However, srp1-49 retained the ability to bind an NLS peptide (26), suggesting that it might be import-proficient. We characterized Sts1 and found that the level of nuclear proteasomes was severely reduced in *sts1-2* (27). The degradation of proteasome substrates was inhibited in *sts1-2* mutant (21, 27, 28), resulting in the accumulation of multiubiquitylated proteins (29). Strikingly, proteasomes are also mislocalized in *srp1-49* (25), and protein degradation is inhibited (25, 28, 30,

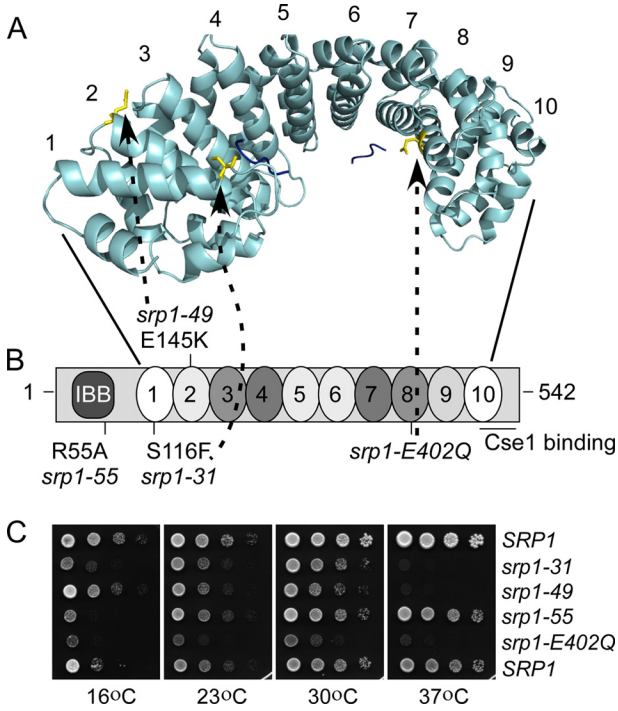

FIGURE 1. **Domain structure of Srp1/importin-α.** *A*, the structure of the array of 10 ARM repeats in the central portion of Srp1 is shown (12), and the position of each repeat motif is indicated. The concave surface contains two NLS binding surfaces. The major NLS pocket is generated by ARM-3 and -4, and the minor NLS is formed by helix-3 residues in ARM-7 and -8. *Small blue lines* represent NLS peptides. The side chains of Ser-116, Glu-145, and Glu-402 are shown in *yellow*. The image in *A* was derived from crystallographic data of Conti *et al.* (12) (Protein Data Bank entry 1BK6) and was prepared using PyMOL (version 1.5.0.4, Schrödinger, LLC, New York). *B*, three key domains in Srp1 are shown in this schematic of the full-length Srp1. *Solid lines* demarcate the region of the protein that is represented in *A*. The amino-terminal IBB domain contains an engineered mutation, R55A, which causes an import defect. The ARM repeat motifs are indicated by *shaded ovals*. The *darker shaded ovals* represent the major (ARM-3 and -4) and minor (ARM-7 and -8) NLS-binding pockets. The carboxyl terminus interacts with Cse1. *C*, the growth defects associated with key mutants are shown. *srp1-31* and *srp1-49* are unable to grow at 37 °C. *srp1-55* showed a pronounced cold temperature growth defect (16 °C). The *srp1-E402Q* mutant showed poor growth at both high and low temperatures.

TABLE 1
Plasmids used in this study

Plasmid	Description	Reference/Source
LEP37	P_{CUP}-*rad4*D C-terminal fragment	Ref. 54
LEP38	P_{CUP}-*rad4*D N-terminal fragment	Ref. 54
LEP796	P_{GAL}-*CLB2*-HA	This study
PUL32	P_{CUP}-*MATα2*-GFP	Ref. 55
pRS426	P_{GAL}-*CDC17*-3HA	Ref. 56
p3349	pRS306-*PUP1*-tDimer-RFP::*URA3*	Ref. 57
LEP263	pBSHU-*RPT1*-GFP-HA	Ref. 58
pRS416	P_{MET25}-Deg1-FLAG-*SEC62*-ProA	Ref. 37
pAC876	pRS-*SRP1*::*CEN*::*URA3*	Ref. 6
pAC1104	pRS-*SRP1*::*CEN*::*LEU2*	Ref. 6
pAC1236	pRS-*srp1-E402Q*::*CEN*::*LEU2*	Ref. 6
LEP843	pRS-*srp1-55*::*CEN*::*LEU2*	This study
pAC592	pRS-*RSL1*::2μ::*TRP1*	Ref. 18
pAC1303	pRS-*CSE1*::2μ::*TRP1*	Ref. 18
pAC1059	P_{MET25}-BPSV40T3-NLS-GFP-GFP	Ref. 20
pAC1065	P_{MET25}-SV40-NLS-GFP-GFP	Ref. 20
pNOY162	pRS-*SRP1*::*CEN*::*TRP1*	Ref. 21
pNOY163	pRS-*srp1-31*::*CEN*::*TRP1*	Ref. 21
pNOY166	pRS-*srp1-49*::*CEN*::*TRP1*	Ref. 21
DEP177	P_{GAL}-*STS1*::2μ	Ref. 59

TABLE 2
Yeast strains used in this study

Strain	Genotype	Reference/Source
NA10	*MAT***a** *ura3-1 trp1-1 ade2-1 leu2-3,112 his3-11 (STS1)*	Ref. 22
NA25	*MAT***a** *ura3-1 trp1-1 ade2-1 leu2-3,112 his3-11 sts1-2* (C194Y)	Ref. 22
NOY388	*MAT***a** *ura3-1 trp1-1 ade2-1 leu2-3,112 his3-11 (SRP1)*	Ref. 21
NOY612	*MATα ura3-1 trp1Δ63 ade2-1 leu2-3,112 his3-11 srp1-31* (S116F)	Ref. 21
NOY613	*MATα ura3-1 trp1Δ63 ade2-1 leu2-3,112 his3-11 srp1-49* (E145K)	Ref. 21
ACY641	*MAT***a** *ura3-52 trp1Δ ade2 leu2Δ1 his3Δ200 srp1-55::LEU2* (R55A)	Ref. 18
ACY324	*MAT***a** *his3Δ200 leu2Δ1 ura3-52 lys2 srp1Δ::HIS3 + SRP1::URA3*	Ref. 19
LCY3084	*MAT***a** *his3Δ200 leu2Δ1 ura3-52 lys2 srp1Δ::HIS3 + SRP1::LEU2* (ACY342 + Srp1)	This study
LCY3085	*MAT***a** *his3Δ200 leu2Δ1 ura3-52 lys2 srp1Δ::HIS3 + srp1-E402Q::LEU2* (ACY342 + srp1-E402Q)	This study
LCY2777	NA10 *(STS1)* + *RPN11*-GFP::*HIS3, PUP1*-RFP::*URA3*	This study
LCY2778	NA25 *(sts1-2)* + *RPN11*-GFP::*HIS3, PUP1*-RFP::*URA3*	This study
LCY3061	NOY388 *(SRP1)* + *RPN11*-GFP::*HIS3, PUP1*-RFP::*URA3*	This study
LCY3063	NOY612 *(srp1-31)* + *RPN11*-GFP::*HIS3, PUP1*-RFP::*URA3*	This study
LCY3065	NOY613 *(srp1-49)* + *RPN11*-GFP::*HIS3, PUP1*-RFP::*URA3*	This study
LCY3067	ACY641 *(srp1-55)* + *RPT1*-GFP::*HIS3*::*URA3*	This study
LCY3095	LCY3084 *(SRP1)* + *RPT1*-GFP::*HIS3*::*URA3*	This study
LCY3098	LCY3084 *(srp1-E402Q)* + *RPT1*-GFP::*HIS3*::*URA3*	This study

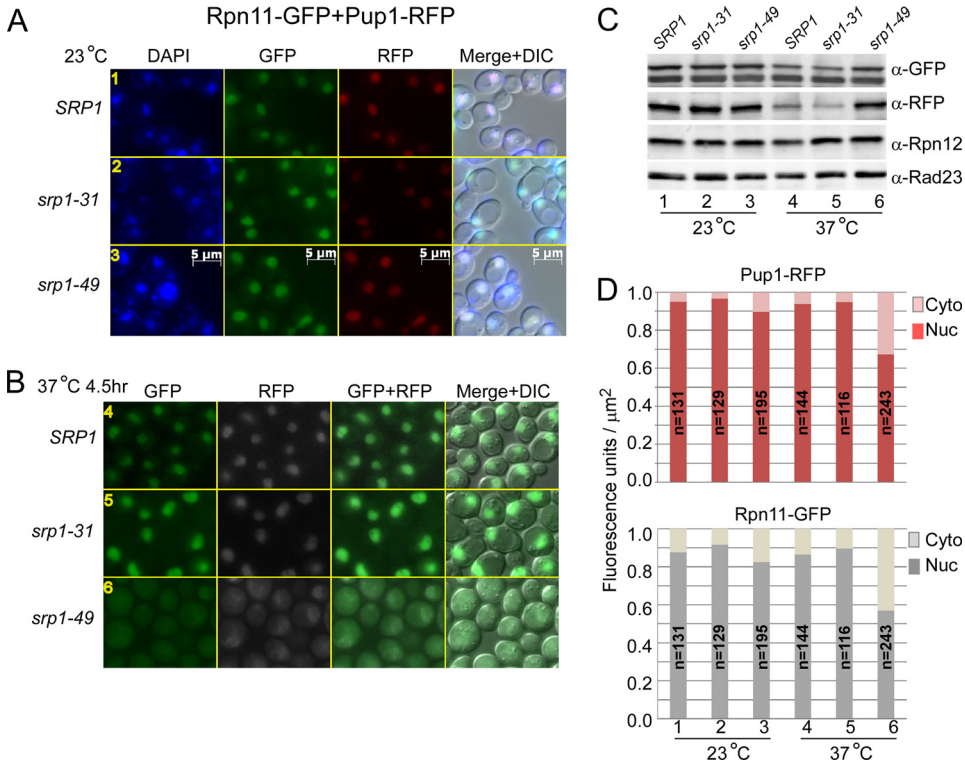

FIGURE 2. **Proteasome mislocalization in *srp1-49*.** *A* and *B*, 19 and 20 S proteasome subunits (Rpn11-GFP and Pup1-RFP, respectively) were expressed at physiological levels in *SRP1*, *srp1-31*, and *srp1-49*. The localization of both proteins was examined in the same field of cells, at the permissive (*A*, 23 °C) and non-permissive (*B*, 37 °C) temperatures. A *merged image* that includes DAPI and differential interference contrast (*DIC*) is shown. *C*, protein extracts were prepared from cultures examined in *A* and *B* to measure Rpn11-GFP and Pup1-RFP protein levels. Antibody reaction against Rpn12 and Rad23 is also shown. *D*, the fluorescence signal from Rpn11-GFP and Pup1-RFP in *A* and *B* was quantified using Zeiss imaging software. Multiple fields were examined, and the total number of cells sampled is indicated *within each bar*. The graph shows the pixel intensity in the nucleus and cytoplasm. An equal intensity in the nucleus and cytosol would be consistent with proteasome mislocalization.

31). We determined that nuclear targeting of proteasomes by Sts1 required an interaction with Srp1 (28). Sts1 formed a weak interaction with the srp1-49 mutant but efficient binding to both Srp1 and srp1-31 proteins (28), thus providing a straightforward explanation for the proteasome targeting defect of *srp1-49*. A protein distantly related to Sts1 in *Schizosaccharomyces pombe* (Cut8) was also found to target proteasome to the nucleus (32).

We determined that overexpression of Sts1 suppressed the proteasome localization defect of *srp1-49* and restored protein degradation. However, Sts1 did not suppress the nuclear import defect of *srp1-31*, demonstrating that it contributes specifically to the proteasome targeting role of Srp1. In agreement, mutations in *STS1* only inhibited proteasome targeting and did not affect nuclear import. We conclude that the proteasome targeting function of Sts1 embodies its involvement in multiple pathways, including cell cycle control, DNA repair, mating pheromone signaling, and DNA replication (28, 29).

The availability of well characterized yeast *srp1* mutants and detailed information on importin-α function offered a unique opportunity to examine the role of Srp1 in proteasome targeting. We specifically investigated whether separate mechanisms were required for nuclear targeting of proteasomes and nuclear import of NLS-containing proteins. We determined that *srp1* mutants that are import-deficient were able to target proteasomes to the nucleus. In contrast, *srp1* mutants that mislocalized proteasomes continued to import nuclear proteins. These findings indicate that proteasome trafficking by Srp1 occurs by a mechanism that is distinct from its well characterized role in the import of nuclear proteins.

EXPERIMENTAL PROCEDURES

Yeast Strains and Plasmids—Yeast strains and plasmids are described in Tables 1 and 2. ACY641 (*srp1-55*), ACY324 (*srp1*Δ::*HIS3* + *SRP1*::*URA3*), pAC1104 (*SRP1*::*LEU2*), pAC1236 (*srp1-E402Q*::*LEU2*), and NLS-GFP were generously provided by Dr. A. Corbett (Emory University, Atlanta, GA) (18, 20). To make *SRP1* and *srp1-E402Q* strains, plasmids pAC1104 and pAC1236 were transformed into ACY324. Transformants were plated on medium containing 5-fluoroorotic acid (5-FOA/*LEU2*), and uracil auxotrophy was confirmed. The growth of cells expressing *srp1-E402Q* was moderately impaired at 30 °C. A plasmid expressing Matα2-GFP was obtained from Dr. Thomas Sommer (Max-Delbruck Center-MDC, Berlin). Deg1-FLAG-Sec62 was obtained from Dr. M. Hochstrasser (Yale University). Materials to integrate Pup1-RFP into the chromosome were provided by Dr. I. Sagot (Université Bordeaux, CNRS). Constructs to integrate Rpt1-GFP were provided by Dr. C. Enenkel (University of Toronto).

Yeast Growth—Wild type and mutant strains were grown at the permissive temperature (23 °C) in selective medium. A culture of exponential phase cells was diluted into selective medium and incubated for 2 h. For temperature shift studies, an aliquot of the culture was first withdrawn at 23 °C. The remain-

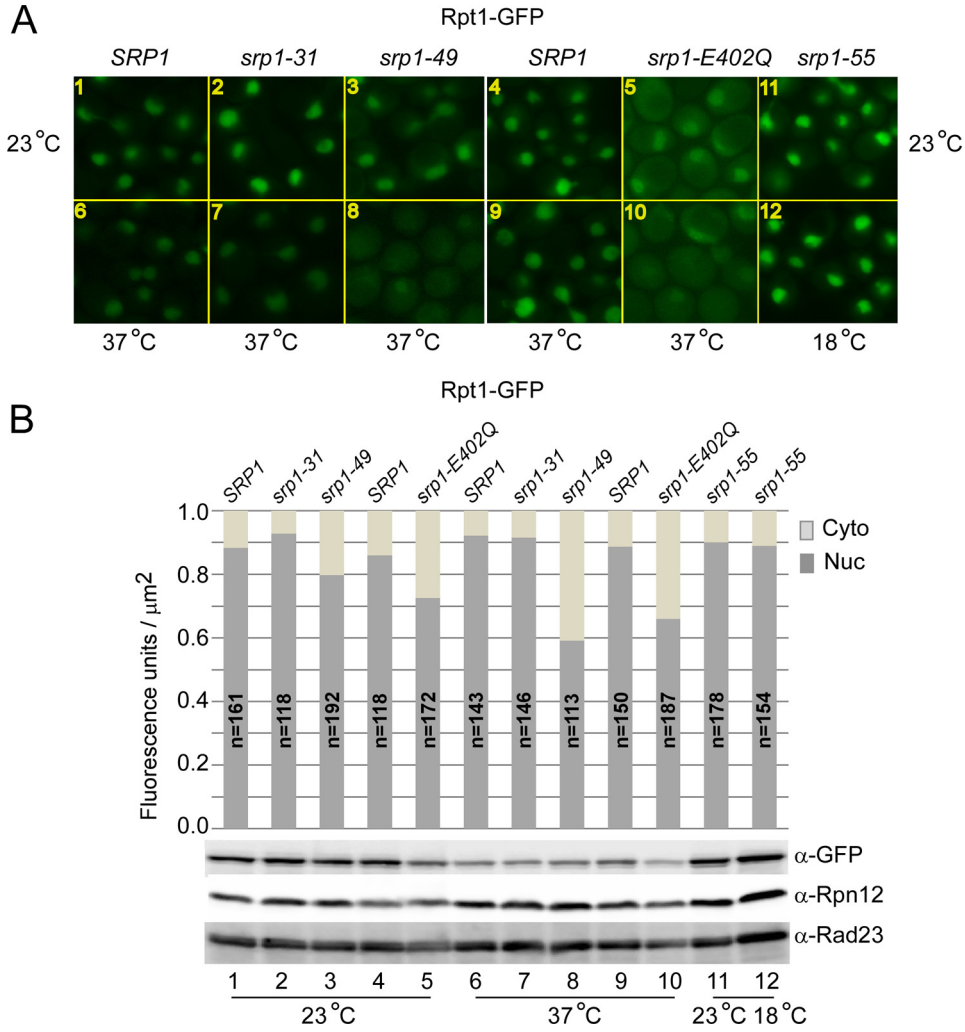

FIGURE 3. ***srp1-E402Q* has a proteasome localization defect.** *A*, the nuclear targeting of Rpt1-GFP was investigated in *srp1*^{E402Q} and *srp1-55*. The temperature-sensitive *srp1*^{E402Q} mutant was examined at 23 and 37 °C, whereas the cold-sensitive *srp1-55* mutant was examined at 23 and 18 °C. *B*, the fluorescence intensity in *A* was quantified. Both *srp1-49* and *srp1-E402Q* showed reduced levels of nuclear proteasomes at 37 °C (*top*). The levels of proteasome subunits Rpt1-GFP and Rpn12 and the shuttle factor Rad23 were determined at the permissive and restrictive temperatures.

der of the culture was resuspended in medium containing cycloheximide (750 μg/ml) and incubated at the non-permissive temperature (either 37 or 18 °C). Samples were analyzed at the times indicated in the figure legends.

Fluorescence Microscopy—Cultures of 500 μl were pelleted, washed in 1 ml of PBS, and suspended in 10 μl of PBS. A 3-μl volume of the cell suspension was spotted on Poly-Prep Slides (Sigma). Fluorescence signal was captured with a Zeiss Imager M1 microscope, using filter set 38HE. All pairwise comparisons between WT and mutant strains were performed using identical exposure settings. The *scale bars* (see Figs. 4 and 10) represent 5 μm.

Preparation of Yeast Lysate, Immunoprecipitation, and Immunoblotting—Yeast cells were suspended in 50 mM Tris, pH 7.5, 150 mM NaCl, 5 mM EDTA, and 1% Triton X-100 (containing protease inhibitors) and lysed by glass bead disruption (Thermo-Savant Fast Prep FP120). Protein extracts were normalized using the Bradford reagent (Bio-Rad). The lysate (50 μg) was resolved in a 12% polyacrylamide SDS-Tricine gel to detect Rad4-HA and Matα2-GFP. Clb2-HA was immunoprecipitated from 2 mg of lysate using anti-HA affinity matrix (Roche Applied Science). The proteins were resolved, transferred to nitrocellulose, and examined by immunoblotting using anti-HA-HRP and anti-GFP antibodies.

Antibodies and Reagents—Polyclonal anti-Rad23 antibody was prepared at Pocono Rabbit Farm and Laboratory, Inc. (Canadensis, PA). Anti-Rpn12 and Rpn10 antibodies were provided by Dr. D. Skowyra (St. Louis University). Monoclonal antibodies against HA was obtained from Roche Applied Science. Polyclonal anti-GFP and anti-ubiquitin antibodies, as well as monoclonal anti-FLAG-HRP antibodies were purchased from Sigma. Enhanced chemiluminescent (ECL) reagents were from PerkinElmer Life Sciences, and the signals were detected and quantified using an Eastman Kodak Co. GelLogic 1500 imaging system and software.

RESULTS

srp1 Mutants Show Unique Allele-specific Defects—We characterized *srp1* mutants to understand how Srp1 targeted proteasomes to the nucleus. The effects of four engineered or genetically derived mutants were examined (Fig. 1, *A* and *B*). The mutation in *srp1-55* resides in the IBB domain (R55A) (19),

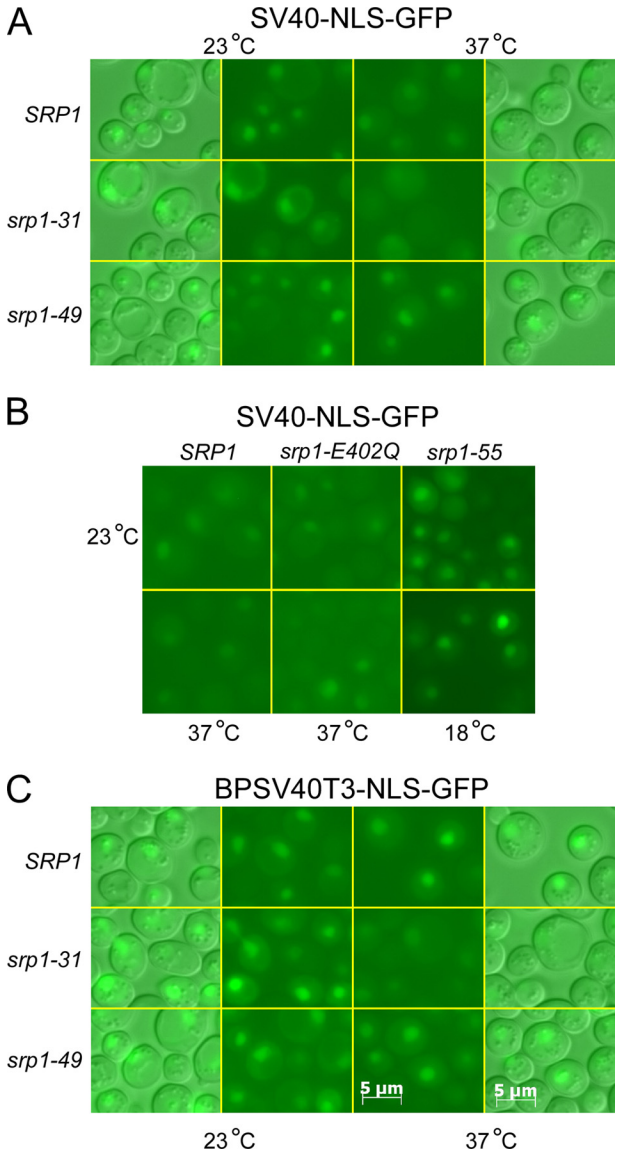

FIGURE 4. **An NLS-containing protein is successfully imported in *srp1-49*.** *A*, SV40-NLS-GFP was detected in the nucleus of *SRP1*, *srp1-31*, and *srp1-49* at the permissive temperature (23 °C). However, after transfer to the non-permissive temperature (37 °C), the level of nuclear SV40-NLS-GFP was significantly reduced in *srp1-31* but not in *SRP1* or *srp1-49*. *B*, the nuclear localization of SV40-NLS-GFP was also examined in *srp1*^{E402Q} and *srp1-55*. *C*, the nuclear import of a reporter protein bearing a bipartite NLS (BPSV40T3-NLS-GFP) was examined in *srp1-31* and *srp1-49*, as described in *A*.

which plays a key role in regulating access to the NLS-binding pocket and also facilitates release of the bound substrate after import. The import defect in *srp1-55* arises from a failure to release cargo proteins following entry into the nucleus (20). The mutation in *srp1-31* also causes a nuclear import defect. The residue that is mutated (S116F) does not contribute directly to binding NLS residues in cargo proteins but is believed to alter the structure of the major NLS-binding pocket (12). The mutation in *srp1-49* is present on the opposite side of the NLS-binding surface. In contrast, *srp1-E402Q* is present on the concave surface and specifically inhibits interaction with the bipartite NLS (12, 20). We confirmed the temperature-sensitive growth defects of *srp1-31* and *srp1-49* mutants at 37 °C (Fig. 1*C*) (11, 33) and the cold temperature growth defect of *srp1-55*. The *srp1-E402Q* mutant showed poor growth at all temperatures tested.

The distribution of a 19 S proteasome subunit (Rpn11-GFP) was examined in *SRP1*, *srp1-31*, and *srp1-49* by fluorescence microscopy (Fig. 2*A*). The localization of Pup1-RFP (a 20 S core subunit) was similarly tested. Both Rpn11-GFP and Pup1-RFP were efficiently localized to the nucleus in *SRP1*, *srp1-31*, and *srp1-49* at the permissive temperature (23 °C). DAPI staining confirmed that the proteasome subunits were co-localized with the nucleus. The same cultures were transferred to 37 °C and examined after 4.5 h (Fig. 2*B*). Proteasome subunits Rpn11-GFP and Pup1-RFP were both efficiently localized to the nucleus in *SRP1* and *srp1-31*. However, neither proteasome subunit was enriched in the nucleus in *srp1-49*. Protein extracts were examined by immunoblotting to determine whether the lack of fluorescence in *srp1-49* reflected proteasome mislocalization and not degradation (Fig. 2*C*). Protein extracts were prepared from the same cells examined microscopically and resolved by SDS-PAGE. An immunoblot was incubated with antibodies against GFP, RFP, Rpn12, and Rad23. The abundance of all four proteins was similar at 23 °C. Similar levels were also observed at 37 °C. The moderately lower level of Pup1-RFP protein in *srp1-31* is consistent with the lower fluorescence in this strain. However, Pup1-RFP was efficiently nucleus-localized in *srp1-31*. More importantly, the levels of three proteasome subunits (Rpn11-GFP, Pup1-RFP, and Rpn12) were similar in *SRP1* and *srp1-49* at 37 °C, confirming that the loss of nuclear fluorescence in *srp1-49* was caused by mislocalization and not degradation.

Fluorescence intensity was quantified in the three strains at both 23 °C and 37 °C (Fig. 2*D*). Fluorescence pixel density was determined in the cytosol and the nucleus from multiple fields of view. The ratio of nuclear/cytosolic distribution of Pup1-RFP and Rpn11-GFP approached equivalence in *srp1-49* at 37 °C, consistent with predominant localization in the cytosol.

To extend these observations, we examined *srp1-E402Q* and *srp1-55* mutants, which harbor distinct defects in nuclear import (20). srp1-E402Q shows defective binding to a bipartite nuclear localization signal, and srp1-55 is unable to efficiently release NLS-containing substrates in the nucleus (20). We expressed the proteasome subunit Rpt1-GFP at physiological levels in *srp1-E402Q* and *srp1-55* and examined its subcellular distribution (Fig. 3*A*). *srp1-55* is a cold-sensitive mutant, and nuclear targeting of proteasomes was compared at 23 and 18 °C (non-permissive condition). Rpt1-GFP was targeted efficiently to the nucleus in *srp1-55* (at 18 °C), similar to *SRP1* and *srp1-31*. In contrast, Rpt1-GFP was significantly mislocalized in *srp1-E402Q* at 37 °C, similar to *srp1-49*. Fluorescence intensity was measured in the cytosol and nucleus (Fig. 3*B*, *top*). We confirmed that the levels of Rpt1-GFP, Rpn12, and Rad23 were essentially unchanged at 37 °C (Fig. 3*B*, *bottom*). A modest decrease in the levels of these proteins in *srp1-E402Q* may be due to the higher fraction of inviable cells. These studies confirmed that the loss of fluorescence signal in the nucleus was due to mislocalization and not protein degradation.

Distinct Import Defects in srp1 Mutants—The failure of srp1-49 and srp1-E402Q to target proteasomes to the nucleus led us to investigate their proficiency in nuclear import. SV40-

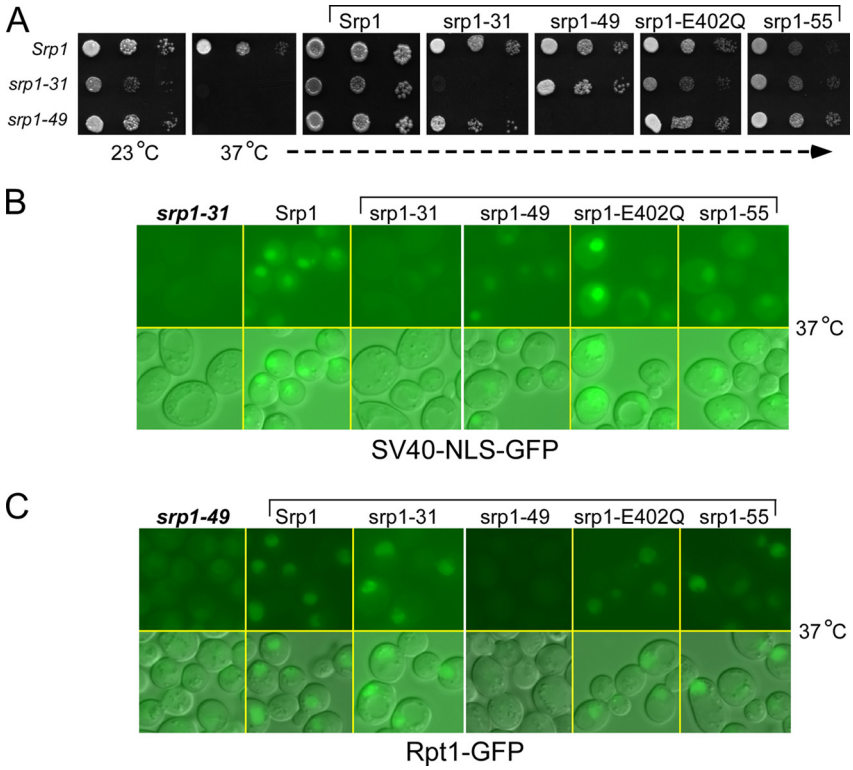

FIGURE 5. **Intragenic complementation by *srp1* alleles.** *SRP1*, *srp1-31*, and *srp1-49* were transformed with plasmids expressing Srp1, srp1-31, srp1-49, srp1-E402Q, and srp1-55. *A*, yeast cells were plated on agar medium and incubated at either 23 or 37 °C. The growth defect of *srp1-31* and *srp1-49* (37 °C; *second panel*) was suppressed by wild type Srp1. The expression of srp1-31 protein restored growth in all mutants except for *srp1-31*. Similarly, only srp1-49 failed to suppress the growth defect of *srp1-49*. The expression of srp1-E402Q and srp1-55 suppressed the temperature-sensitive growth defects of both *srp1-31* and *srp1-49*. *B*, the inability of *srp1-31* to import SV40-NLS-GFP was suppressed by all srp1 mutant proteins except for srp1-31. *C*, the proteasome targeting defect of *srp1-49* was restored by all srp1 mutant proteins except for srp1-49. As expected, wild type Srp1 suppressed the NLS import and proteasome targeting defects of *srp1-31* and *srp1-49*, respectively.

NLS-GFP is an engineered protein whose entry into the nucleus is readily observed. SV40-NLS-GFP was enriched in the nucleus in wild type (*SRP1*), *srp1-31* and *srp1-49* mutants at 23 °C (Fig. 4*A*). As expected, after transfer to 37 °C, nuclear import of SV40-NLS-GFP ceased in *srp1-31*. Surprisingly, nuclear import of SV40-NLS-GFP was not affected in *srp1-49*. NLS-mediated import was also examined in *srp1-55* and *srp1-E402Q* (Fig. 4*B*). Despite the severe proteasome targeting defect in *srp1-E402Q* (Fig. 3*A*), SV40-NLS-GFP was efficiently imported. We also examined the import of BPSV40-NLS-GFP, a reporter bearing the bipartite nuclear targeting sequence (Fig. 4*C*). BPSV40-NLS-GFP was imported into the nucleus in *SRP1* and *srp1-49* at both permissive and non-permissive temperatures, whereas a moderate import deficiency was seen in *srp1-31* (Fig. 4*C*).

Nuclear Localization of a Proteasome Subunit (Rpt1) Is Restored by Intragenic Complementation—The temperature-sensitive growth defect of *srp1-31* and *srp1-49* was confirmed (Fig. 5*A*). Wild type Srp1 restored growth of *srp1-31* and *srp1-49* at 37 °C. The temperature-sensitive growth defects of *srp1-31* and *srp1-49* were overcome when both mutant proteins were co-expressed (Fig. 5*A*) (21). Specifically, the growth of *srp1-49* at 37 °C was restored by expression of all derivatives of Srp1, except srp1-49. Similarly, the growth defect of *srp1-31* was restored by each srp1 mutant protein except srp1-31. However, the mechanism underlying intragenic complementation had not been investigated.

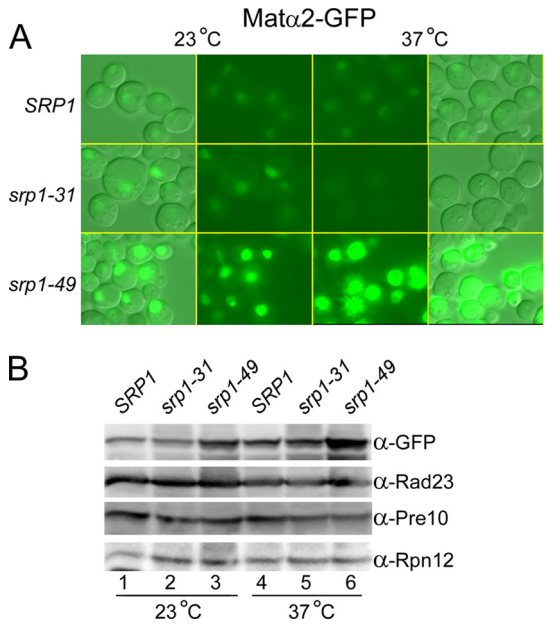

FIGURE 6. **Proteasome mislocalization in *srp1-49* stabilizes Matα2-GFP.** *A*, Matα2-GFP was examined in *SRP1*, *srp1-31*, and *srp1-49* at 23 and 37 °C. High level of Matα2-GFP was detected in *srp1-49* at 23 °C. Matα2-GFP levels increased significantly at 37 °C. *B*, extracts were prepared from the cultures examined in *A* and characterized by immunoblotting. Anti-GFP antibodies confirmed elevated levels of Matα2-GFP in *srp1-49*. The levels of proteasome subunits Pre10 and Rpn12 were unaffected.

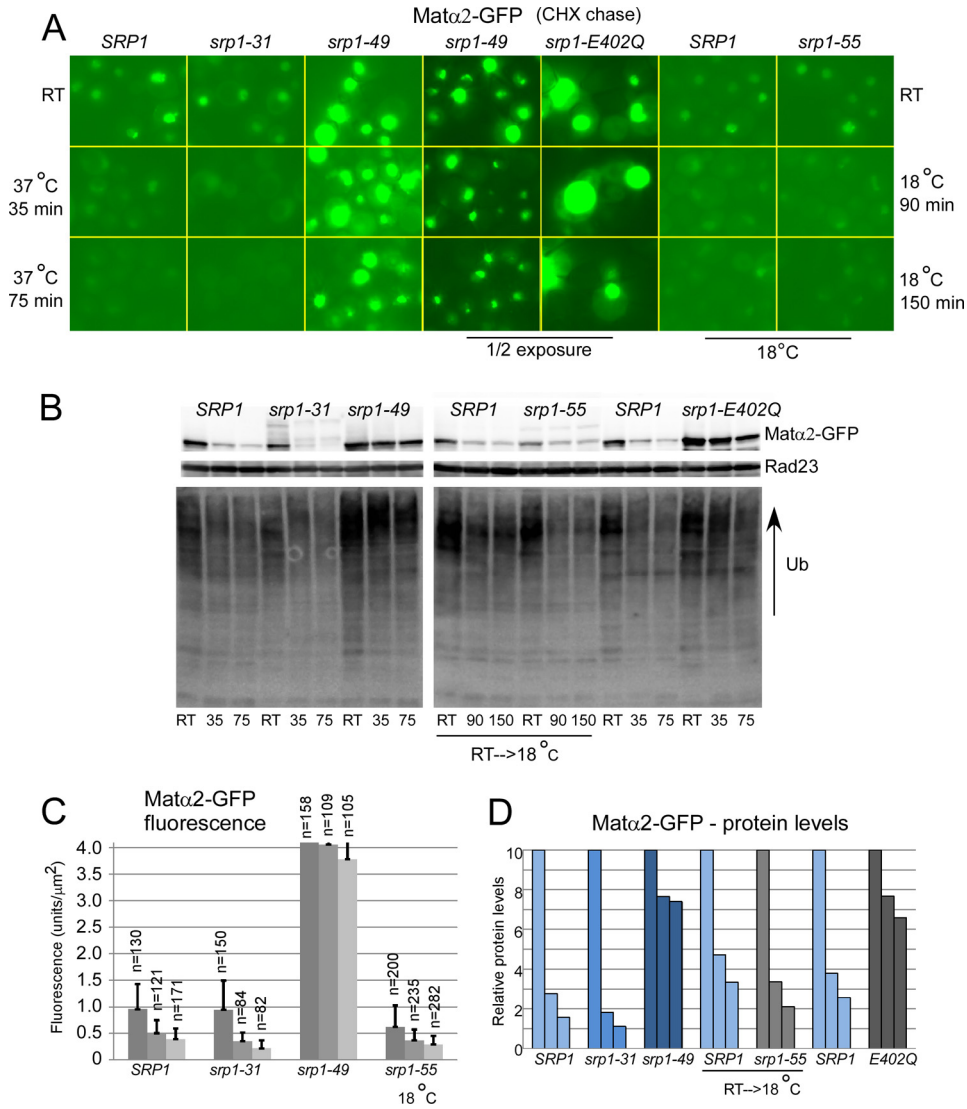

FIGURE 7. **Proteasomes mislocalization inhibits the turnover of Matα2-GFP in *srp1-E402Q*.** *A*, Matα2-GFP was expressed in *srp1-E402Q* and *srp1-49*, and dramatic nuclear accumulation was observed at both 23 and 37 °C. A reduced exposure (*1/2 exposure*) is shown. The degradation of Matα2-GFP was not affected in *srp1-55* (at 18 °C). *B*, extracts were prepared from the cultures described in *A*, and Matα2-GFP levels were measured by immunoblotting. Matα2-GFP protein levels decreased rapidly in *SRP1*, *srp1-31* (at 37 °C), and *srp1-55* (at 18 °C), but were stable in *srp1-49* and *srp1-E402Q*. The elimination of multiubiquitylated proteins was delayed in both *srp1-49* and *srp1-E402Q*. Rad23 levels were similar in all strains. *C*, the level of Matα2-GFP in *A* was quantified in multiple fields, and the number of cells characterized in each strain is indicated. (The level of Matα2-GFP in *srp1-E402Q* was not determined due to the high signal.) *D*, the level of Matα2-GFP protein in *B* was quantified by densitometry, and the zero time for each strain was set to an arbitrary value of 10. *CHX*, cycloheximide.

We determined that all srp1 mutant proteins, except srp1-31, could restore nuclear import of SV40-NLS-GFP in *srp1-31* (Fig. 5*B*). In a reciprocal study, we found that all srp1 mutants restored nuclear targeting of proteasome subunit Rpt1-GFP in *srp1-49* except srp1-49 (Fig. 5*C*). These *trans*-complementation studies indicate that NLS-mediated import occurs by a mechanism distinct from the targeting of proteasomes to the nucleus.

The Stabilization of a Nuclear Substrate in srp1 Mutants Is Allele-specific—Matα2 is a well studied transcription regulator that is degraded by the ubiquitin/proteasome system (34). At the permissive temperature (23 °C) Matα2-GFP was detected in the nucleus in *SRP1, srp1–31,* and *srp1-49* (Fig. 6*A*). However, markedly higher levels were present in the nucleus in *srp1-49*, suggesting that proteasome mislocalization occurs even at the permissive temperature. The nuclear accumulation of Matα2-GFP increased dramatically at 37 °C in *srp1-49*. We measured Matα2-GFP protein levels and confirmed higher levels in *srp1-49* at both 23 °C (Fig. 6*B*, *lane 3*) and 37 °C (*lane 6*). In contrast, the levels of proteasome subunits Pre10 and Rpn12 as well as the shuttle-factor Rad23 were essentially unchanged. We note that at 37 °C, Matα2-GFP is not detected in the nucleus of *srp1-31* because of its severe import defect (Fig. 6*A*). However, the abundance of Matα2-GFP was similar to that of the wild type strain, indicating that it was present in the cytosol.

A time-based assay was used to examine Matα2-GFP levels. We blocked protein synthesis and observed rapid depletion of Matα2-GFP in *SRP1* and *srp1-31* (Fig. 7*A*). In contrast, Matα2-GFP fluorescence was high in *srp1-49* at 23 °C and remained elevated for 75 min at 37 °C. A reduced exposure (Fig. 7*A*, *1/2 exposure*) confirmed the striking accumulation of Matα2-GFP in the nucleus of *srp1-49*. Matα2-GFP fluorescence also dimin-

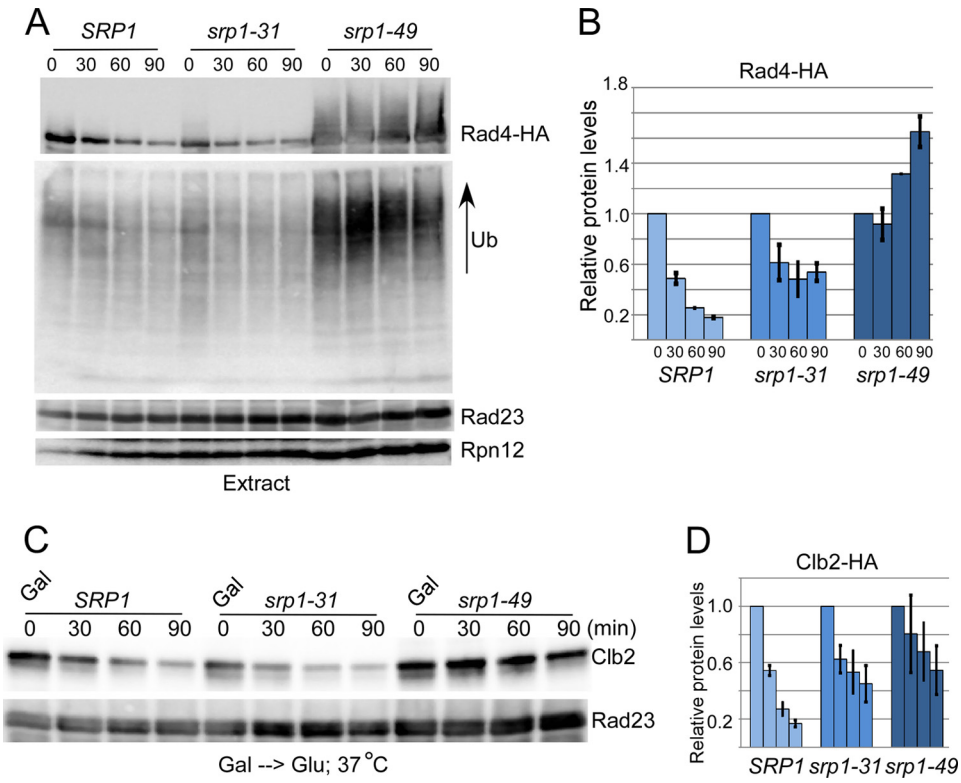

FIGURE 8. **Proteasome mislocalization stabilizes DNA repair and cell-cycle factors**. *A*, the turnover of the nucleotide excision repair factor Rad4-HA was determined in *SRP1*, *srp1-31*, and *srp1-49*, following the addition of cycloheximide. The reactions to antibodies against the HA epitope, ubiquitin (*Ub*), Rad23, and proteasome subunit Rpn12 are shown. *B*, Rad4-HA levels were quantified by densitometry, and the level in each strain was compared with its individual zero time point. *C*, Clb2-HA was expressed from a galactose-inducible promoter (P_{GAL1}) in *SRP1*, *srp1-31*, and *srp1-49*. Protein levels were examined after the cells were transferred from inducing (*Gal*) to repressive (*Glu*) medium at 37 °C and quantified (*D*) as described above.

ished rapidly in *srp1-55*, reflecting efficient nuclear targeting of proteasomes in this mutant. However, Matα2-GFP levels increased dramatically in *srp1-E402Q*, causing difficulty in obtaining an exposure within the dynamic range.

We verified that the GFP fluorescence seen in Fig. 7*A* reflected higher Matα2-GFP protein abundance (Fig. 7*B*). Immunoblotting showed that Matα2-GFP was stabilized in both *srp1-49* and *srp1-E402Q*. We measured the levels of multiubiquitylated proteins and detected higher levels in *srp1-49* and *srp1-E402Q* (Fig. 7*B*, *bottom*). The stabilization of Matα2-GFP in Fig. 7*B* was quantified by densitometry (Fig. 7*D*). The fluorescence signal in Fig. 7*A* was also quantified (Fig. 7*C*). These results suggest that the failure to translocate proteasomes to the nucleus in *srp1-49* and *srp1-E402Q* will cause stabilization of nuclear substrates.

We measured the turnover of additional nuclear proteins, including the DNA repair protein Rad4 (29, 35) and the mitotic cyclin Clb2 (29, 36). Rad4-HA was degraded in both *SRP1* and *srp1-31* (Fig. 8*A*) but was strongly stabilized in *srp1-49*. Significant accumulation of high molecular weight ubiquitylated proteins (Fig. 8, *Ub*) was confirmed in *srp1-49*, whereas the levels of Rad23 and proteasome subunit Rpn12 were unchanged. Rad4-HA levels were quantified by densitometry, and data compiled from three independent experiments are shown (Fig. 8*B*). The stability of Clb2-HA was similarly examined in *SRP1*, *srp1-31*, and *srp1-49*, and significant stabilization was detected in *srp1-49* (Fig. 8*C*) and quantified (Fig. 8*D*).

Failure to Degrade Matα2-GFP Causes Nuclear Accumulation—We reported previously that Sts1 binds Srp1 to target proteasomes to the nucleus (28). Because Matα2-GFP is stabilized when proteasomes are mislocalized in *srp1-49* and *srp1-E402Q*, a similar effect was predicted to occur in *sts1-2*. Matα2-GFP was expressed in *sts1-2*, and its subcellular distribution was examined after cells were transferred from 23 to 37 °C. Cycloheximide was added to the medium to inhibit further synthesis of Matα2-GFP. Initial levels of Matα2-GFP were noticeably higher in *sts1-2* at the permissive temperature (Fig. 9*A*, *panel 6*) and are consistent with our findings in *srp1-49* (Fig. 7*A*). After transfer to 37 °C, Matα2-GFP was rapidly eliminated in *STS1*, as noted by the loss of nuclear fluorescence (0-, 25-, 45-, and 75-min chase). In contrast, Matα2-GFP levels were essentially unchanged in *sts1-2*. After 75 min, Matα2-GFP was undetectable in *STS1*, but nuclear levels were still present in *sts1-2*. The fluorescence intensity was quantified (Fig. 9*B*). We examined extracts by immunoblotting and confirmed that Matα2-GFP was rapidly degraded in *STS1* but was stable in *sts1-2* (Fig. 9*C*, *top*). These data were quantified by densitometry (Fig. 9*C*, *bottom*).

A failure to target proteasomes to the nucleus in either *sts1* or *srp1* mutants inhibits the degradation of nuclear proteins. We therefore questioned whether defects in proteasome function would also cause nuclear accumulation of proteolytic substrates. We expressed Matα2-GFP in *RPN11* and *rpn11-1* and examined protein levels at permissive (23 °C) and non-permis-

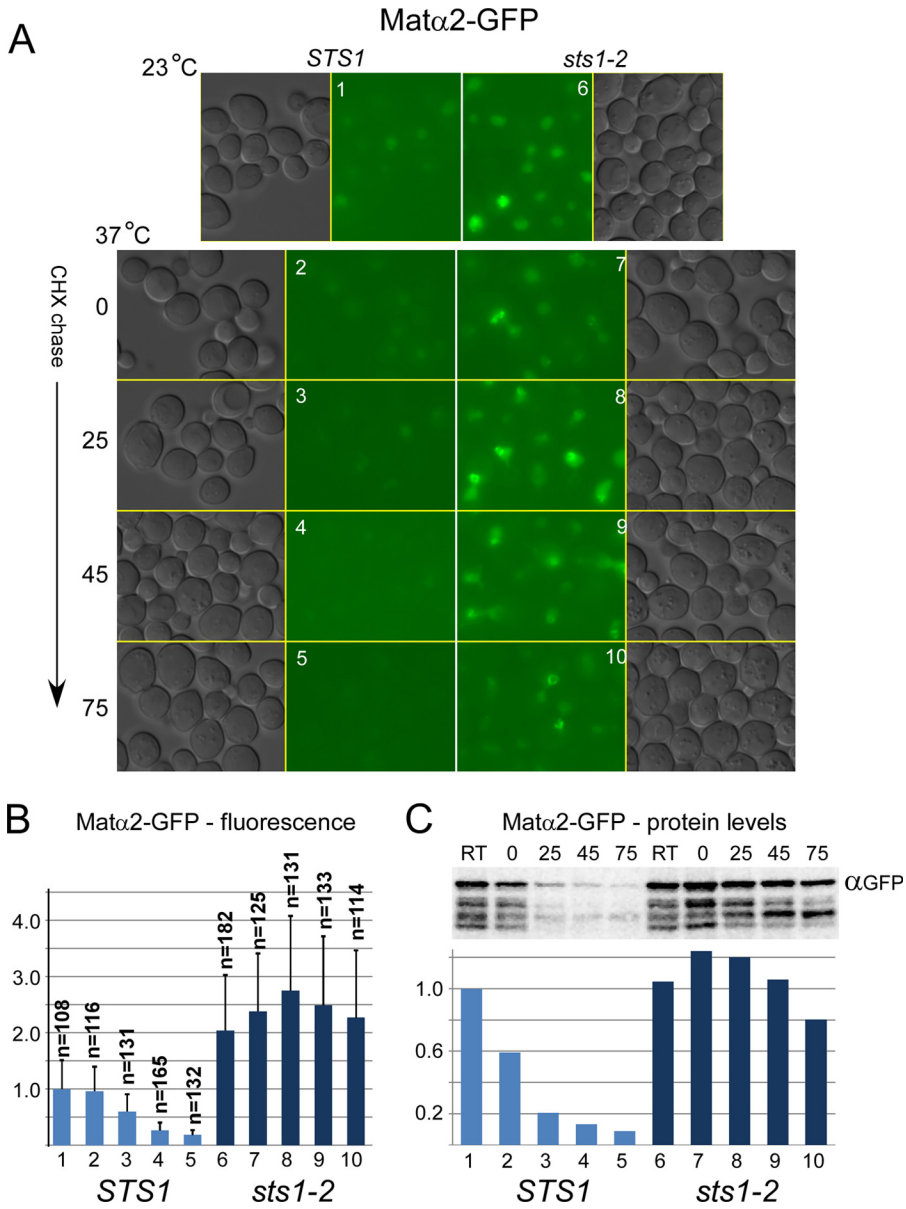

FIGURE 9. **A proteasome substrate accumulates in the nucleus in *sts1-2*.** *A*, Matα2-GFP was expressed in *STS1* and *sts1-2* at 23 °C. The cultures were resuspended in fresh medium containing cycloheximide and incubated at 37 °C. The GFP signal was lost rapidly in *STS1* but remained elevated in *sts1-2*. *B*, Matα2-GFP fluorescence was measured in multiple fields, and the number of cells examined is indicated. *C*, protein extracts were prepared from the same samples described in *A* and characterized by immunoblotting (*top*). Matα2-GFP levels were quantified by densitometry and standardized to the level detected at time 0.

sive (37 °C) temperatures (Fig. 10*A*). Similar levels of Matα2-GFP were detected at 23 °C. However, Matα2-GFP levels increased dramatically in *rpn11-1* at 37 °C.

Proteasomes in *sts1-2* are mislocalized within 30 min after cells are transferred to 37 °C. We investigated whether Matα2-GFP would be rapidly stabilized in *rpn11-1* after transfer to 37 °C. Higher levels of Matα2-GFP were seen in *rpn11-1* at 23 °C (Fig. 10*B*). GFP fluorescence increased rapidly in *rpn11-1* after transfer to 37 °C, and the accumulation of Matα2-GFP protein and multiubiquitylated proteins was confirmed (Fig. 10*C*). Matα2-GFP also accumulated in proteasome mutants *rpt1*/*cim5-1* and *pre1-1 pre2-2* (Fig. 10*D*). *pre1-1 pre2-2* is not temperature-sensitive (*ts*) for growth, and higher levels of Matα2-GFP were seen at both 23 and 37 °C. *rpt1* has a temperature-sensitive growth defect, and higher levels of Matα2-GFP were seen predominantly at 37 °C.

Srp1 Specifically Affects the Turnover of Nuclear Proteins—FLAG-Deg1-Sec62 is an engineered, endoplasmic reticulum-associated protein that is degraded by cytosolic proteasomes (37). FLAG-Deg1-Sec62 was efficiently degraded in *SRP1*, *srp1-31*, *srp1-49*, *srp1-E402Q*, and *srp1-55* mutants (Fig. 11). However, FLAG-Deg1-Sec62 was strongly stabilized in *pre1-1 pre2-2*, confirming its turnover by cytosolic proteasomes and demonstrating that Srp1 only affects the turnover of nuclear proteins.

Overexpression of Sts1 Restored Normal Growth and Protein Degradation in srp1-49—Tabb *et al.* (21) found that Sts1 could suppress the growth defect of *srp1-49* but not *srp1-31*, reinforc-

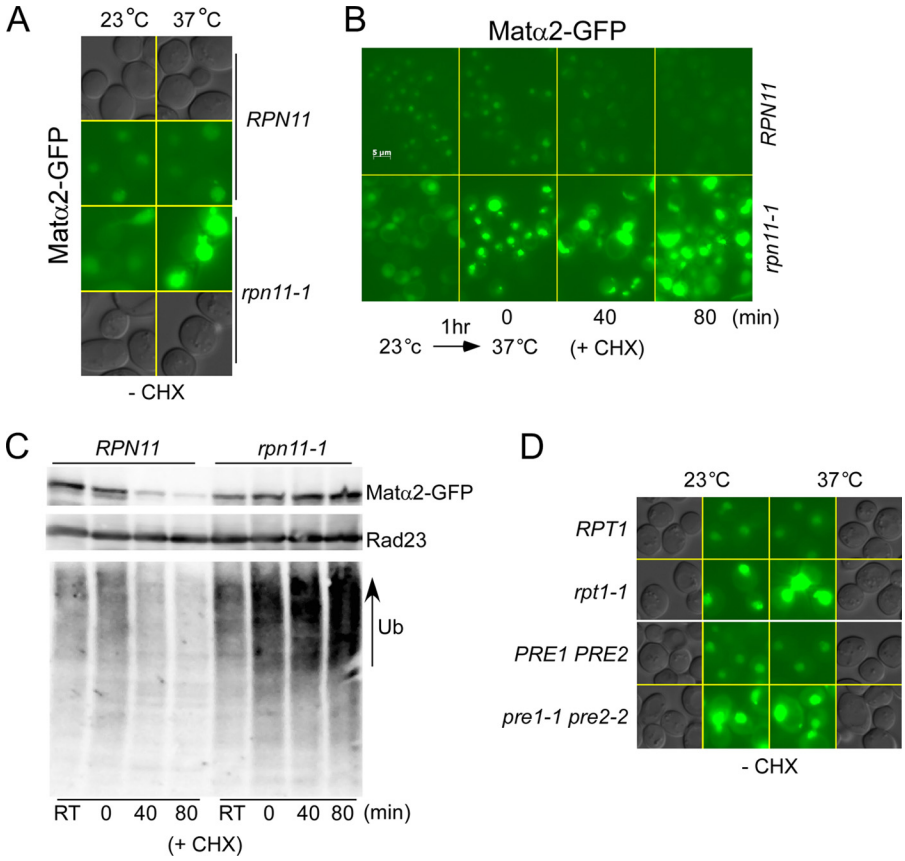

FIGURE 10. **A proteolytic substrate accumulates in the nucleus in proteasome mutants.** *A*, Matα2-GFP was expressed in *RPN11* and *rpn11-1*, and its localization was examined at 23 and 37 °C. *B*, the same yeast cultures were transferred from 23 to 37 °C for 1 h, after which cycloheximide (*CHX*) was added to the medium, and aliquots were withdrawn at the times indicated. *C*, extracts were prepared from the cultures examined in *B* and characterized by immunoblotting. The stabilization of Matα2-GFP in *rpn11-1* was accompanied by dramatic accumulation of high molecular weight ubiquitylated species. *D*, Matα2-GFP was stabilized in other proteasome mutants (*rpt1/cim5-1* and *pre1-1 pre2-2*) and accumulated in the nucleus.

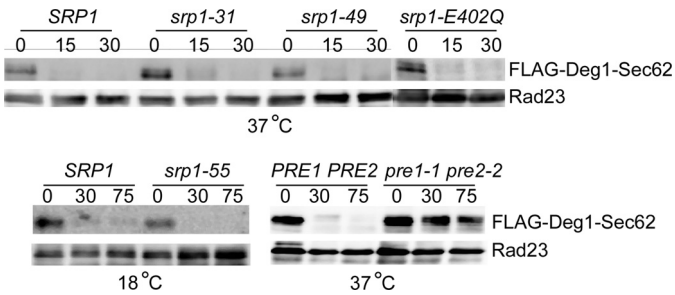

FIGURE 11. **Srp1 does not affect the proteasome-mediated degradation of a cytosolic protein.** FLAG-Deg1-Sec62 was expressed in *srp1* mutants, and protein extracts were prepared at the times indicated. An immunoblot was incubated with antibodies against the FLAG epitope and Rad23. FLAG-Deg1-Sec62 stability was also examined in wild type (*PRE1 PRE2*) and *pre1-1 pre2-2* proteasome mutant.

ing the idea that Srp1 has two biochemically distinct functions. To determine whether an interaction between Sts1 and Srp1 was required for suppressing the growth defect of *srp1-49*, we examined $^{\Delta NLS}$sts1, which lacks an Srp1-binding motif (28). The $^{\Delta NLS}$sts1 mutant failed to suppress the growth defect of *srp1-49* (Fig. 12*A*), demonstrating that the Srp1/Sts1 interaction is required for growth at 37 °C. In contrast, overexpression of Sts1 in *srp1-49* re-established nuclear localization of proteasomes (Fig. 12*B*, *Rpt1-GFP*) but did not suppress the import deficiency of *srp1-31* (data not shown). Overexpression of Sts1 had no adverse effect on the targeting of Rpt1-GFP in *srp1-31* and *SRP1*. By restoring proteasome targeting to the nucleus, Sts1 overexpression also restored Matα2-GFP degradation in *srp1-49* (Fig. 12*C*). We conclude that the targeting of proteasomes to the nucleus by Srp1 and Sts1 involves a mechanism that is distinct from the import of NLS-containing proteins.

DISCUSSION

Multiple pathways promote nuclear import, and a well characterized mechanism involves the importin-α/β heterodimer. In yeast, importin-α is encoded by *SRP1*, and its role in NLS-mediated protein import has been characterized extensively (20, 38, 39). Srp1 also performs a poorly understood role in protein degradation that is generally believed to involve its nuclear import activity (21, 25).

We found that the protein degradation function of Srp1 requires its interaction with Sts1 (28). Sts1 performs a key role in targeting proteasomes to the nucleus (28). Mutations in both Srp1 and Sts1 can cause proteasome mislocalization, which inhibits protein degradation. A distantly related protein in *S. pombe* (Cut8) can also guide proteasomes to the nuclear surface (32, 40). Blm10 was recently reported to traffic proteasome core particles to the nucleus (41). However, Blm10 operates independently of Srp1 and is not required for viability. In contrast, Sts1 is essential for viability, suggesting that it mediates a major pathway for proteasome localization.

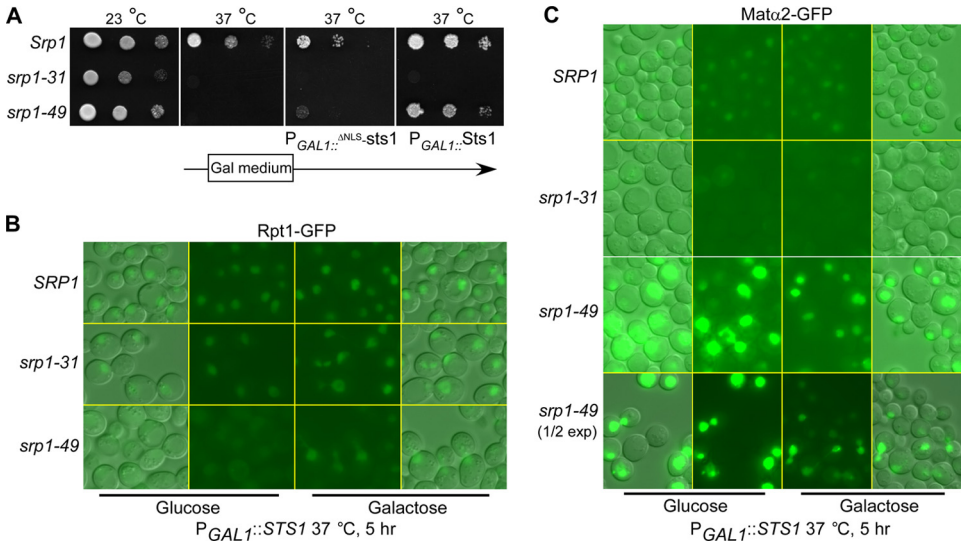

FIGURE 12. **Srp1/Sts1 interaction is required for suppression of *srp1-49*.** *A*, Sts1 and $^{\Delta NLS}$sts1 were expressed from the galactose-inducible P_{GAL1} promoter in *SRP1*, *srp1-31*, and *srp1-49*. 10-fold serial dilutions were spotted on agar medium, and growth was examined on galactose medium at 23 and 37 °C. *B*, Rpt1-GFP localization was examined at 37 °C on glucose (*left*) and galactose (*right*) media in *SRP1*, *srp1-31*, and *srp1-49* overexpressing Sts1. *C*, Matα2-GFP and P_{GAL1}::*STS1* were co-expressed in *SRP1*, *srp1-31*, and *srp1-49*. Overexpression of Sts1 (galactose) resumed degradation of Matα2-GFP, as indicated by the loss of GFP signal. (A reduced exposure is also shown.)

The presence of NLS motifs in certain proteasome subunits suggests that they may be imported directly through an interaction with Srp1 (29). A bipartite NLS in Rpn2 was shown to target a reporter protein to the nucleus (25). We note that proteasome subcomplexes can operate in the nucleus (31, 42), although they perform non-proteolytic roles (43, 44). It is significant that peptidase activity has not been convincingly demonstrated in the nucleus. The import of proteasome subcomplexes that perform non-proteolytic functions could be different from the localization of proteasomes by Sts1 that promotes degradation. None of the proteasome subunits that were mislocalized in *sts1-2* contained identifiable NLS motifs.

We identified two types of *srp1* mutants that are either unable to import NLS-containing proteins (*srp1-31* and *srp1-55*) or fail to target proteasomes to the nucleus (*srp1-49* and *srp1-E402Q*). These are distinct and non-overlapping functions because co-expression of *srp1-31* and *srp1-49* mutants resulted in intragenic complementation. Specifically, the expression of srp1-31 protein in *srp1-49* restored nuclear targeting of proteasomes and Matα2 degradation. Similarly, nuclear import resumed in *srp1-31* when srp1-49 was co-expressed (Fig. 5). Overexpression of Sts1 suppressed the growth defect of *srp1-49* (21) but not *srp1-31*, reinforcing the view that Srp1 has multiple roles.

The biochemical basis for proteasome mislocalization in *srp1-49* is probably due to its weak interaction with Sts1 (28). In contrast, Sts1 formed an efficient interaction with srp1-31, and nuclear localization of proteasomes is proficient in *srp1-31*. Intra-allelic complementation can be explained by the formation of a dimer. Although Tabb *et al.* (21) had speculated that Srp1 functioned as a monomer, we note that the structure of Srp1 revealed a homodimer in the crystal (12). The formation of a Srp1/Srp1 dimer is also suggested by the complementation observed by co-expressing *srp1-49* and *srp1-E402Q*, which are both defective in proteasome targeting (Fig. 5*C*). Further study will be required to confirm the existence and functional relevance of an Srp1/Srp1 dimer.

Several *srp1* mutants that we examined have been well characterized (20, 21, 25). To strengthen our hypothesis that Srp1 performs two different roles, we characterized *srp1-55* and *srp1-E402Q*, which have unique defects in nuclear import (18, 19, 20). The srp1-55 mutant contains an alanine substitution of Arg-55 (see Fig. 1), which inhibits the release of NLS cargo (20). SV40-GFP-NLS was localized to the nucleus in *srp1-55*, because its defect occurs after nuclear entry. Proteasomes were efficiently targeted to the nucleus in *srp1-55*, and the turnover of a nuclear protein was not affected. In contrast, *srp1-E402Q* failed to target proteasomes to the nucleus (Fig. 3*B*) and caused striking stabilization of a nuclear substrate (Fig. 7*A*).

The mutations in Srp1 that cause proteasome mislocalization (E145K and E402Q) are spatially distant. Glu-145 is present in ARM-2 but lies on the opposite side of the NLS binding surface (12). Therefore, it is not surprising that srp1-49 successfully imported NLS-containing proteins. However, srp1-49 formed a weak interaction with Sts1, suggesting that this region of Srp1 might be important for binding regulatory factors such as Sts1. Glu-402 is located in the middle of helix-3 of ARM-8 and is present in the concave NLS-binding surface of Srp1. Pulliam *et al.* (20) showed that srp1-E402Q is defective in binding a bipartite NLS motif.

Tabb *et al.* (21) identified two clusters of closely juxtaposed basis residues in Sts1. Disruption of the first cluster partially reduced nuclear localization of Sts1, suggesting a requirement for an additional targeting motif. We characterized the Sts1 protein sequence using cNLS-Mapper, a tool designed to search for NLS motifs (45). cNLS-Mapper identified a bipartite NLS that included both clusters of basic residues detected previously by Tabb *et al.* (21). The proteasome targeting defect of srp1-E402Q might be due to its inability to bind a putative bipartite NLS in Sts1.

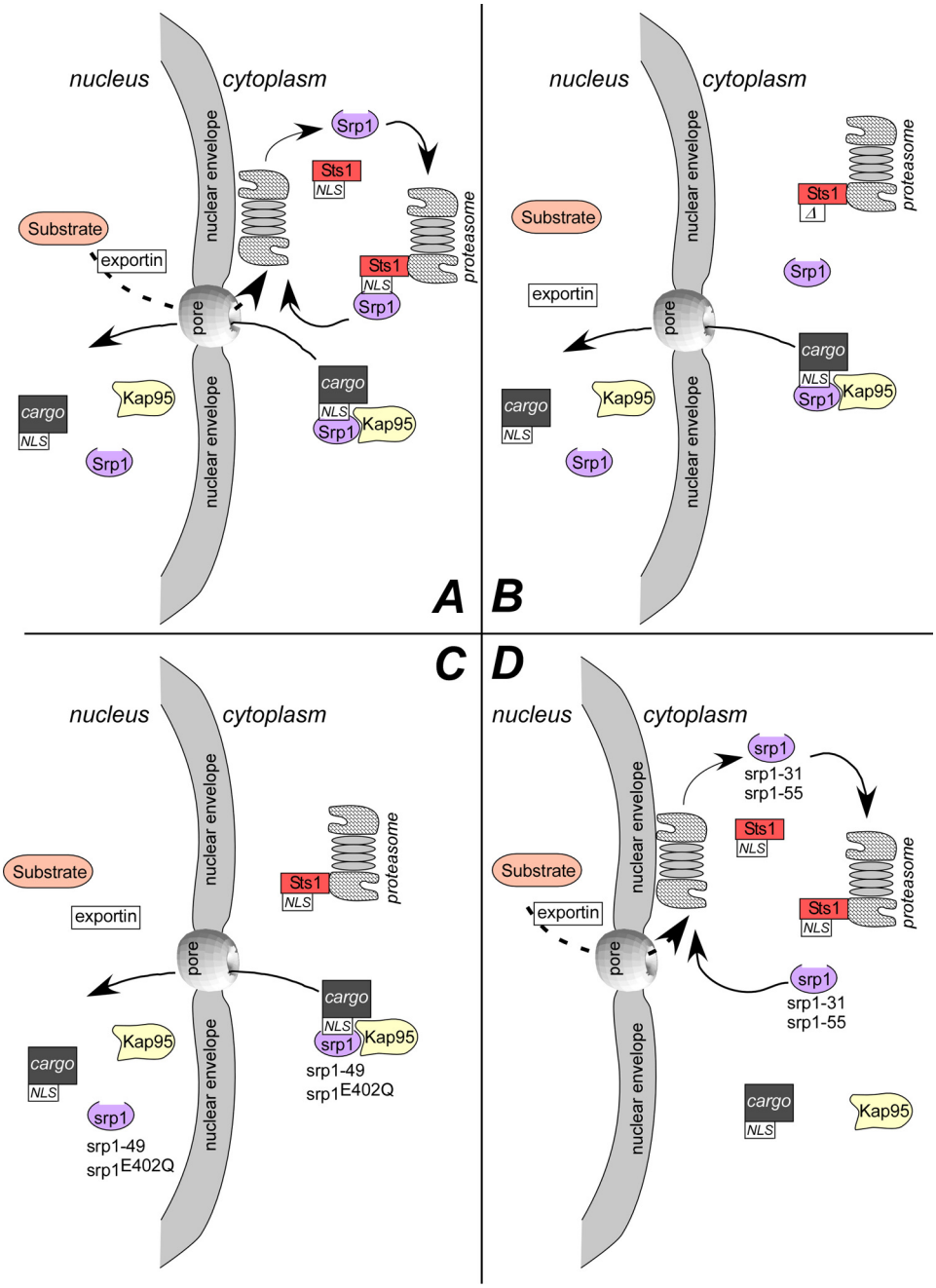

FIGURE 13. **A model for Srp1 function**. *A*, we propose that in wild type cells, Sts1 binds Srp1 to translocate proteasomes to the nucleus. Proteasomes at the nuclear surface may receive nuclear substrates that are exported. A separate activity of Srp1 is to import NLS-containing proteins (*cargo*), which we presume occurs concurrently with the nuclear targeting of proteasomes. NLS-mediated import requires Srp1 interactions with other import factors (such as Kap85/importin-*β*). *B*, a mutation in Sts1 that prevents interaction with Srp1 ($^{\Delta NLS}$sts1) prevents the translocation of proteasomes to the nucleus and causes stabilization and nuclear accumulation of proteins (28). However, the nuclear import of other NLS-containing proteins is not affected by Sts1. *C*, certain mutations in Srp1 (*srp1-49* and *srp1-E402Q*) prevent nuclear targeting of proteasomes. However, *srp1-49* and *srp1-E402Q* mutants are proficient in importing cNLS-containing proteins. Proteolytic substrates accumulate inside the nucleus in these mutants. One interpretation of this result is that nuclear substrates are not exported unless proteasomes are available at the nuclear surface. *D*, the prototypical *srp1* mutants, embodied by srp1-31, failed to import NLS-containing proteins. However, these mutants could target proteasomes to the nucleus, allowing successful degradation of nuclear substrates.

The mutation in *srp1-31* replaces serine with phenylalanine (S116F). Serine 116 is located in ARM-1, which lies at the boundary of the NLS-binding pocket. ARM-1 does not contribute directly to binding NLS but is likely to affect the structural integrity of the importin-α NLS-binding surface (12). *srp1-31* showed a severe defect in importing a monopartite NLS (SV40-GFP-NLS). However, srp1-31 only showed a moderate defect in importing bipartite NLS (Fig. 4; BPSV40T3-GFP-NLS). We showed previously that srp1-31 forms an efficient interaction with Sts1 (28), consistent with the idea that a bipartite NLS in Sts1 binds the minor NLS motif in Srp1. However, further study will be required to determine whether Sts1 contains a bipartite NLS.

A requirement for importin-α in stress response was reported to be distinct from its function in importing NLS-containing proteins (17). Importin-α was also found to restrict

the import of specific transcription factors (16), underscoring unique and unexpected functions for this nuclear transporter. Similarly, we report that Srp1 function in targeting proteasomes to the nucleus is exclusive from its action in importing NLS-containing proteins. We speculate that Sts1 diverts Srp1 from its nuclear import function to promote nuclear localization of proteasomes. There is evidence that proteasome subunits are enriched in the nuclear envelope (11, 31, 46, 47).

Both regulatory and misfolded nuclear proteins are ubiquitylated and degraded by the proteasome (48–50). Whereas the ligation of ubiquitin to nuclear proteins has been described, the site of their degradation has not been examined systematically. Indeed, there is no compelling evidence that intact 26 S proteasomes and peptidase activity are present in the nucleus. The degradation of nuclear proteins is inhibited in both *srp1-49* and *sts1-2* (Fig. 7*B*), consistent with the proteasome-targeting defect in these mutants (25, 28). However, the rapid stabilization of nuclear substrates in *srp1-49*, *srp1-E402Q*, and *sts1-2* was surprising because nuclear substrates should have been degraded if proteasomes had entered prior to the shift to nonpermissive temperature. This was not observed, suggesting a scarcity of catalytically active proteasomes inside the nucleus. In agreement with this view, we recently reported that many nuclear proteins are degraded by cytosolic proteasomes after export, in agreement with other studies (29, 51, 52). The degradation of cytoplasmic proteins was not affected in either *srp1-49* or *sts1-2* (Fig. 11), demonstrating that the accumulation of multiubiquitylated proteins in these mutants (29) represent nuclear proteins.

We propose that Srp1 is engaged concurrently in importing nuclear proteins and localizing proteasomes to the nucleus (see model in Fig. 13*A*). However, a mutation that disrupts Srp1/Sts1 interaction (srp1-49; $sts1^{\Delta NLS}$) specifically inhibits proteasome targeting without affecting NLS-mediated import. Nuclear substrates that are stabilized in *srp1-49*, *srp1-E402Q*, and *sts1-2* accumulate inside the nucleus (Fig. 13*B*). In contrast, mutations in Srp1 that inhibit delivery of NLS cargo (srp1-31 and srp1-55) do not prevent the nuclear targeting of proteasomes (Fig. 13*D*).

It is presently not known whether Srp1/Sts1 import proteasomes into the nucleus or merely guide them to the nuclear surface. We speculate that proteasomes are located on the nuclear surface because the export pathway is required for degrading multiple nuclear substrates (29, 53). Our studies do not rule out the degradation of specific proteins within the nucleus, although the significant accumulation of multiubiquitylated proteins in export mutants (28) indicates that the export pathway plays an important role in nuclear protein turnover. Further study will be required to establish the location of catalytically active proteasomes, the site of nuclear protein degradation, and the specific involvement of the export mechanism.

Acknowledgments—We thank Drs. A. Corbett, C. Enenkel, M. Hochstrasser, I. Sagot, D. Skowyra, and S. Wente for plasmids, strains, and antibodies. We thank D. Nandakumar for assistance with Fig. 1A. We thank K. Marshall, E. Okeke, and M. Meadow for critical review of the manuscript.

REFERENCES

1. Kaffman, A., and O'Shea, E. K. (1999) Regulation of nuclear localization: a key to a door. *Annu. Rev. Cell Dev. Biol.* **15,** 291–339
2. Lee, S. J., Matsuura, Y., Liu, S. M., and Stewart, M. (2005) Structural basis for nuclear import complex dissociation by RanGTP. *Nature* **435,** 693–696
3. Bayliss, R., Corbett, A. H., and Stewart, M. (2000) The molecular mechanism of transport of macromolecules through nuclear pore complexes. *Traffic* **1,** 448–456
4. Suntharalingam, M., and Wente, S. R. (2003) Peering through the pore: nuclear pore complex structure, assembly, and function. *Dev. Cell* **4,** 775–789
5. Kalderon, D., Roberts, B. L., Richardson, W. D., and Smith, A. E. (1984) A short amino acid sequence able to specify nuclear location. *Cell* **39,** 499–509
6. Leung, S. W., Harreman, M. T., Hodel, M. R., Hodel, A. E., and Corbett, A. H. (2003) Dissection of the karyopherin α nuclear localization signal (NLS)-binding groove: functional requirements for NLS binding. *J. Biol. Chem.* **278,** 41947–41953
7. Yano, R., Oakes, M. L., Tabb, M. M., and Nomura, M. (1994) Yeast Srp1p has homology to armadillo/plakoglobin/β-catenin and participates in apparently multiple nuclear functions, including the maintenance of the nucleolar structure. *Proc. Natl. Acad. Sci. U.S.A.* **91,** 6880–6884
8. Enenkel, C., Blobel, G., and Rexach, M. (1995) Identification of a yeast karyopherin heterodimer that targets import substrate to mammalian nuclear pore complexes. *J. Biol. Chem.* **270,** 16499–16502
9. Pemberton, L. F., Blobel, G., and Rosenblum, J. S. (1998) Transport routes through the nuclear pore complex. *Curr. Opin. Cell Biol.* **10,** 392–399
10. Ryan, K. J., McCaffery, J. M., and Wente, S. R. (2003) The Ran GTPase cycle is required for yeast nuclear pore complex assembly. *J. Cell Biol.* **160,** 1041–1053
11. Yano, R., Oakes, M., Yamaghishi, M., Dodd, J. A., and Nomura, M. (1992) Cloning and characterization of SRP1, a suppressor of temperature-sensitive RNA polymerase I mutations, in *Saccharomyces cerevisiae*. *Mol. Cell Biol.* **12,** 5640–5651
12. Conti, E., Uy, M., Leighton, L., Blobel, G., and Kuriyan, J. (1998) Crystallographic analysis of the recognition of a nuclear localization signal by the nuclear import factor karyopherin α. *Cell* **94,** 193–204
13. Kobe, B. (1999) Autoinhibition by an internal nuclear localization signal revealed by the crystal structure of mammalian importin α. *Nat. Struct. Biol.* **6,** 388–397
14. Gilchrist, D., Mykytka, B., and Rexach, M. (2002) Accelerating the rate of disassembly of karyopherin·cargo complexes. *J. Biol. Chem.* **277,** 18161–18172
15. Moroianu, J., Blobel, G., and Radu, A. (1996) The binding site of karyopherin alpha for karyopherin β overlaps with a nuclear localization sequence. *Proc. Natl. Acad. Sci. U.S.A.* **93,** 6572–6576
16. Yasuhara, N., Yamagishi, R., Arai, Y., Mehmood, R., Kimoto, C., Fujita, T., Touma, K., Kaneko, A., Kamikawa, Y., Moriyama, T., Yanagida, T., Kaneko, H., and Yoneda, Y. (2013) Importin α subtypes determine differential transcription factor localization in embryonic stem cells maintenance. *Dev. Cell* **26,** 123–135
17. Young, J. C., Ly-Huynh, J. D., Lescesen, H., Miyamoto, Y., Browne, C., Yoneda, Y., Koopman, P., Loveland, K. L., and Jans, D. A. (2013) The nuclear import factor importin α4 can protect against oxidative stress. *Biochim. Biophys. Acta* **1833,** 2348–2356
18. Harreman, M. T., Hodel, M. R., Fanara, P., Hodel, A. E., and Corbett, A. H. (2003) The auto-inhibitory function of importin α is essential *in vivo*. *J. Biol. Chem.* **278,** 5854–5863
19. Harreman, M. T., Cohen, P. E., Hodel, M. R., Truscott, G. J., Corbett, A. H., and Hodel, A. E. (2003) Characterization of the auto-inhibitory sequence within the N-terminal domain of importin α. *J. Biol. Chem.* **278,** 21361–21369
20. Pulliam, K. F., Fasken, M. B., McLane, L. M., Pulliam, J. V., and Corbett, A. H. (2009) The classical nuclear localization signal receptor, importin-α, is required for efficient transition through the G_1/S stage of the cell cycle in *Saccharomyces cerevisiae*. *Genetics* **181,** 105–118

21. Tabb, M. M., Tongaonkar, P., Vu, L., and Nomura, M. (2000) Evidence for separable functions of Srp1p, the yeast homolog of importin α (Karyopherin α): role for Srp1p and Sts1p in protein degradation. *Mol. Cell Biol.* **20,** 6062–6073
22. Amrani, N., Dufour, M. E., Bonneaud, N., and Lacroute, F. (1996) Mutations in STS1 suppress the defect in 3′ mRNA processing caused by the rna15-2 mutation in *Saccharomyces cerevisiae*. *Mol. Gen. Genet.* **252,** 552–562
23. Liang, S., Lacroute, F., and Képès, F. (1993) Multicopy STS1 restores both protein transport and ribosomal RNA stability in a new yeast sec23 mutant allele. *Eur. J. Cell Biol.* **62,** 270–281
24. Houman, F., and Holm, C. (1994) DBF8, an essential gene required for efficient chromosome segregation in *Saccharomyces cerevisiae*. *Mol. Cell Biol.* **14,** 6350–6360
25. Wendler, P., Lehmann, A., Janek, K., Baumgart, S., and Enenkel, C. (2004) The bipartite nuclear localization sequence of Rpn2 is required for nuclear import of proteasomal base complexes via karyopherin αβ and proteasome functions. *J. Biol. Chem.* **279,** 37751–37762
26. Shulga, N., Roberts, P., Gu, Z., Spitz, L., Tabb, M. M., Nomura, M., and Goldfarb, D. S. (1996) *In vivo* nuclear transport kinetics in *Saccharomyces cerevisiae*: a role for heat shock protein 70 during targeting and translocation. *J. Cell Biol.* **135,** 329–339
27. Romero-Perez, L., Chen, L., Lambertson, D., and Madura, K. (2007) Sts1 can overcome the loss of Rad23 and Rpn10 and represents a novel regulator of the ubiquitin/proteasome pathway. *J. Biol. Chem.* **282,** 35574–35582
28. Chen, L., Romero, L., Chuang, S. M., Tournier, V., Joshi, K. K., Lee, J. A., Kovvali, G., and Madura, K. (2011) Sts1 plays a key role in targeting proteasomes to the nucleus. *J. Biol. Chem.* **286,** 3104–3118
29. Chen, L., and Madura, K. (2014) Degradation of specific nuclear proteins occurs in the cytoplasm in *Saccharomyces cerevisiae*. *Genetics* **197,** 193–197
30. Isono, E., Nishihara, K., Saeki, Y., Yashiroda, H., Kamata, N., Ge, L., Ueda, T., Kikuchi, Y., Tanaka, K., Nakano, A., and Toh-e, A. (2007) The assembly pathway of the 19 S regulatory particle of the yeast 26 S proteasome. *Mol. Biol. Cell* **18,** 569–580
31. Lehmann, A., Janek, K., Braun, B., Kloetzel, P. M., and Enenkel, C. (2002) 20 S proteasomes are imported as precursor complexes into the nucleus of yeast. *J. Mol. Biol.* **317,** 401–413
32. Takeda, K., and Yanagida, M. (2005) Regulation of nuclear proteasome by Rhp6/Ubc2 through ubiquitination and destruction of the sensor and anchor Cut8. *Cell* **122,** 393–405
33. Loeb, J. D., Schlenstedt, G., Pellman, D., Kornitzer, D., Silver, P. A., and Fink, G. R. (1995) The yeast nuclear import receptor is required for mitosis. *Proc. Natl. Acad. Sci. U.S.A.* **92,** 7647–7651
34. Hochstrasser, M., Ellison, M. J., Chau, V., and Varshavsky, A. (1991) The short-lived MAT α 2 transcriptional regulator is ubiquitinated *in vivo*. *Proc. Natl. Acad. Sci. U.S.A.* **88,** 4606–4610
35. Ortolan, T. G., Chen, L., Tongaonkar, P., and Madura, K. (2004) Rad23 stabilizes Rad4 from degradation by the Ub/proteasome pathway. *Nucleic Acids Res.* **32,** 6490–6500
36. Hood, J. K., Hwang, W. W., and Silver, P. A. (2001) The *Saccharomyces cerevisiae* cyclin Clb2p is targeted to multiple subcellular locations by cis- and trans-acting determinants. *J. Cell Sci.* **114,** 589–597
37. Rubenstein, E. M., Kreft, S. G., Greenblatt, W., Swanson, R., and Hochstrasser, M. (2012) Aberrant substrate engagement of the ER translocon triggers degradation by the Hrd1 ubiquitin ligase. *J. Cell Biol.* **197,** 761–773
38. Miyamoto, Y., Hieda, M., Harreman, M. T., Fukumoto, M., Saiwaki, T., Hodel, A. E., Corbett, A. H., and Yoneda, Y. (2002) Importin α can migrate into the nucleus in an importin β- and Ran-independent manner. *EMBO J.* **21,** 5833–5842
39. Wu, J., Corbett, A. H., and Berland, K. M. (2009) The intracellular mobility of nuclear import receptors and NLS cargoes. *Biophys. J.* **96,** 3840–3849
40. Takeda, K., Tonthat, N. K., Glover, T., Xu, W., Koonin, E. V., Yanagida, M., and Schumacher, M. A. (2011) Implications for proteasome nuclear localization revealed by the structure of the nuclear proteasome tether protein Cut8. *Proc. Natl. Acad. Sci. U.S.A.* **108,** 16950–16955
41. Weberruss, M. H., Savulescu, A. F., Jando, J., Bissinger, T., Harel, A., Glickman, M. H., and Enenkel, C. (2013) Blm10 facilitates nuclear import of proteasome core particles. *EMBO J.* **32,** 2697–2707
42. Gillette, T. G., Huang, W., Russell, S. J., Reed, S. H., Johnston, S. A., and Friedberg, E. C. (2001) The 19 S complex of the proteasome regulates nucleotide excision repair in yeast. *Genes Dev.* **15,** 1528–1539
43. Russell, S. J., Reed, S. H., Huang, W., Friedberg, E. C., and Johnston, S. A. (1999) The 19 S regulatory complex of the proteasome functions independently of proteolysis in nucleotide excision repair. *Mol. Cell* **3,** 687–695
44. Xie, Y., and Varshavsky, A. (2001) RPN4 is a ligand, substrate, and transcriptional regulator of the 26 S proteasome: a negative feedback circuit. *Proc. Natl. Acad. Sci. U.S.A.* **98,** 3056–3061
45. Kosugi, S., Hasebe, M., Tomita, M., and Yanagawa, H. (2009) Systematic identification of cell cycle-dependent yeast nucleocytoplasmic shuttling proteins by prediction of composite motifs. *Proc. Natl. Acad. Sci. U.S.A.* **106,** 10171–10176
46. Niepel, M., Molloy, K. R., Williams, R., Farr, J. C., Meinema, A. C., Vecchietti, N., Cristea, I. M., Chait, B. T., Rout, M. P., and Strambio-De-Castillia, C. (2013) The nuclear basket proteins Mlp1p and Mlp2p are part of a dynamic interactome including Esc1p and the proteasome. *Mol. Biol. Cell* **24,** 3920–3938
47. Scott, C. M., Kruse, K. B., Schmidt, B. Z., Perlmutter, D. H., McCracken, A. A., and Brodsky, J. L. (2007) ADD66, a gene involved in the endoplasmic reticulum-associated degradation of α-1-antitrypsin-Z in yeast, facilitates proteasome activity and assembly. *Mol. Biol. Cell* **18,** 3776–3787
48. Blondel, M., Galan, J. M., Chi, Y., Lafourcade, C., Longaretti, C., Deshaies, R. J., and Peter, M. (2000) Nuclear-specific degradation of Far1 is controlled by the localization of the F-box protein Cdc4. *EMBO J.* **19,** 6085–6097
49. Gardner, R. G., Nelson, Z. W., and Gottschling, D. E. (2005) Degradation-mediated protein quality control in the nucleus. *Cell* **120,** 803–815
50. Garrenton, L. S., Braunwarth, A., Irniger, S., Hurt, E., Künzler, M., and Thorner, J. (2009) Nucleus-specific and cell cycle-regulated degradation of mitogen-activated protein kinase scaffold protein Ste5 contributes to the control of signaling competence. *Mol. Cell Biol.* **29,** 582–601
51. Freedman, D. A., and Levine, A. J. (1998) Nuclear export is required for degradation of endogenous p53 by MDM2 and human papillomavirus E6. *Mol. Cell Biol.* **18,** 7288–7293
52. Lahaye, F., Lespinasse, F., Staccini, P., Palin, L., Paquis-Flucklinger, V., and Santucci-Darmanin, S. (2010) hMSH5 is a nucleocytoplasmic shuttling protein whose stability depends on its subcellular localization. *Nucleic Acids Res.* **38,** 3655–3671
53. Lommel, L., Ortolan, T., Chen, L., Madura, K., and Sweder, K. S. (2002) Proteolysis of a nucleotide excision repair protein by the 26 S proteasome. *Curr. Genet.* **42,** 9–20
54. Schauber, C., Chen, L., Tongaonkar, P., Vega, I., Lambertson, D., Potts, W., and Madura, K. (1998) Rad23 links DNA repair to the ubiquitin/proteasome pathway. *Nature* **391,** 715–718
55. Lenk, U., and Sommer, T. (2000) Ubiquitin-mediated proteolysis of a short-lived regulatory protein depends on its cellular localization. *J. Biol. Chem.* **275,** 39403–39410
56. Ricke, R. M., and Bielinsky, A. K. (2004) Mcm10 regulates the stability and chromatin association of DNA polymerase-α. *Mol. Cell* **16,** 173–185
57. Laporte, D., Salin, B., Daignan-Fornier, B., and Sagot, I. (2008) Reversible cytoplasmic localization of the proteasome in quiescent yeast cells. *J. Cell Biol.* **181,** 737–745
58. Enenkel, C., Lehmann, A., and Kloetzel, P. M. (1998) Subcellular distribution of proteasomes implicates a major location of protein degradation in the nuclear envelope-ER network in yeast. *EMBO J.* **17,** 6144–6154
59. Chen, L., and Madura, K. (2002) Rad23 promotes the targeting of proteolytic substrates to the proteasome. *Mol. Cell Biol.* **22,** 4902–4913